Shahid Beheshti University

Journal of Gems & Precious Metals

Journal homepage: http://gem.sbu.ac.ir

BET testing method for Neyshabour low-grade turquoise, NE of Iran

Mohammad Reza Akrami*[a], Mohammad Yazdi[a], Saeed Nojavan[a]

[a] Department of Geology, Faculty of Earth Science, Shahid Beheshti University, Iran

ARTICLE INFO

Keywords:
BET method
Surface area
Turquoise
Neyshabour
Iran

Article history:
Received: 22 Sep 2020
Accepted: 29 Nov 2020

*corresponding author.
E-mail address:
mo.akrami@mail.sbu.ac.ir
(M.R. Akrami)

ABSTRACT

BET method is based on the absorption of some specific molecular species in a gaseous state based on their surface. This method is used to measure physical absorption which can be used for analyzing the structure of porous materials. BET data show the geometrical shape of porosity, absorption and porosity type, volume, and size of specific surface area. The instrumental methods show that the exact contents of fluids (gas or liquid) can be absorbed by the porous material surface, at different pressures, in different materials such as gemstones. BET method is used to measure physical absorption and analyzing the structure of low-grade Neyshabour turquoise as a base for their chemical treatment. The low-grade turquoises were deposited as gangue for centuries in the area. The treatment of low-grade turquoise provides a good economic opportunity to upgrade the gemological industry in the area. This research would provide a useful framework for further steps such as finding the best turquoise for treatment as well as identifying treated samples from other turquoise sources. The result of the analysis in this research shows that the geometrical shape of porosity is two sided and from an open cylindrical type. The porosity is mainly micro-pore type ($P_0 \leq 0.5$) and the absorption grade as high type. As a result, liquids could penetrate the low-grade turquoise rock pieces and make it possible to consider the low-grade types for further chemical treatment studies.

1. Introduction

Iran has a great potential for gemstones, including turquoise, in terms of diversity and unique geological features. Persian turquoise has been well known in the world since antiquity. Turquoise is one of the famous and oldest known gemstones of Iran. It was initially named by Iranians “pērōzah” meaning “victory”, and later the Arabs called it “fayrūzah”, which is pronounced in Modern Persian as “fīrūzeh”. In Iranian architecture, the blue turquoise was used to cover the domes of palaces because its intense blue color was also a symbol of heaven on earth (Mortimer, 1746; Afshar, 2004; Ghorbani, 2003; Hajalilu, 2007). During history, the turquoise became a symbol for Iranian culture (Pogue, 1915; Hazen, 1984; Reyahi, 1963). People have used it as a symbol God’s blessings accompanying them, if they have a piece of it on their finger (ring), neck (necklace), or arm (bracelets) (King, 2002; Isfahani Sheikh, 1860; Sotoodeh, 1954). Turquoise reserves can be found in different parts of the world. But Iran has been an important source and trade center of turquoise for at least 2000 years. This can be attributed to its unique color, easy cutting, and extensive trade, due to Iran being located on the Silk Road (Akrami et al., 2019; 2020; Yazdi, 2008.) Since 7000 years ago, turquoise has been extracted from Neyshabour mine in NE of Iran. The mine is located 55 km NW of the city of Neyshabour. The city was founded in the 3rd century by the Sassanid dynasty as a provincial capital.

It later became the capital of different Islamic dynasties during 830 to 1037 AD. In this period, it was a significant cultural, commercial, and intellectual center within the Islamic world. During these times turquoise mining was the major mining activity in the area. History of old mining activity in the area has been proven to go back to 4360 BC (Garajian and Lotfi, 2014; Zalinski, 1907; Zavosh, 1969). With new mining activity in 1850, gunpowder was used for the first time in the mines and increased the mining speed. However, by lessening the size of extracted turquoises their value decreased dramatically. Up to the end of the Safavid dynasty, the mines were extracted under the supervision of the government and were stable enough to extend the mining activity till the rise of Qajar dynasty. At the end of the Qajar dynasty, almost all the mines were totally filled by water and rocks and Persian Turquoise lost its position in world markets (Ovissi et al., 2015; 2017). There are numerous old sites, different sections at the mine, that include multi-shaped and various tunnels, which some are still operational (Ovissi et al., 2015). A great deal of research has been done on high-quality turquoise in the country but studies on low-grade turquoises are few. Low-grade turquoises were deposited as gangue and useless parts not only in the Neyshabour mine, but also other turquoise mines. Treatment of the low-grade turquoise provides a good economic opportunity to upgrade the gemological industry mining activities in the area. This research (BET method) would provide a suitable background for further steps such as finding the best turquoise for treatment, as well as identifying treated samples from other turquoise sources . BET is derived from the first letter of three scientists: Brunauer Stephen, Emmett Paul Hug, and Teller Edward who put forward this theory in 1938. The system works by measuring the volume of Nitrogen gas absorbed and desorbed by the surface of the material at disposal of liquid nitrogen at a constant temperature (77 ° K = -196.15 ° C). Before performing the sample surface process, fluid and gases like water, carbon dioxide must be removed. For this purpose, a series of processes including heating, vacuuming, and gas flowing are used (Gibson et al., 2020). In this research, the porosity, specific surface area, and geometrical shape of the cavities of two low-grade turquoise samples are investigated using the BET method. The BET diagram is also called the isothermal absorption and desorption diagram. It is a linear diagram from which the effective surface area of a substance is extracted. There are several types of research and publication about turquoise gemology and it's mining. The following research is the latest one in which the BET method is used to measure physical absorption and analyzing the structure of the Neyshabour turquoise. The result of the BET would be used for low-grade turquoise treatments. Before, low-grade turquoises were deposited as gangue and useless materials for centuries in the mine.

1.1. Geology of the area

From the geological point of view, Neyshabour turquoise mine is located in the Binaloud zone. It is located in the eastern part of the Alborz geotectonic zone at NE of Iran. The area is located in the northeast corner of the 1:100000 geological map of Soltanabad (Fig. 1) (Rezaei et al., 2016; Baumann et al., 1984; Spies et al., 1983; Akrami and Asgari, 2000). The Binalud zone (range) was formed mainly in the Miocene and the Pliocene, during the Alpine orogeny and is made predominantly of Triassic, Jurassic and Eocene volcanic rocks. The southern part of the range was mainly formed by Eocene volcanic rocks. The well-known Neyshabour turquoise comes from the trachytes and andesites of the Eocene volcanic rocks of this part of the mountain range. The volcanic rocks mainly consist of trachyte, andesite, basaltic- andesite, and basalt which are associated with the sedimentary and volcano- sedimentary rocks including limestone, tuff, and breccia. The alteration is hosted in andesitic layers that include silicification, carbonization, propylitization, and to a lesser extent, argillicization and sericitization. Silicification and carbonization are the most important alterations in the area which are associated with turquoise mineralization (Karimpour et al., 2012).

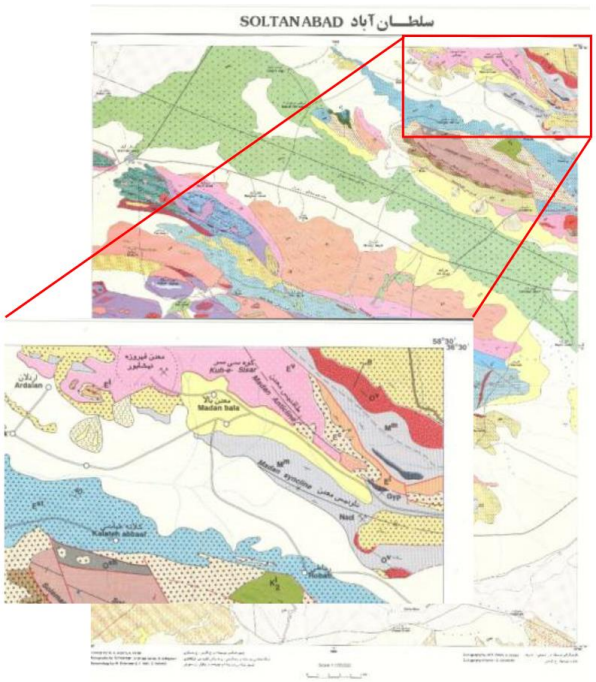

Fig. 1. 1:100000 geological map of Soltanabad (Akrami et al., 2000)

Turquoise mineralization mainly occurs in Eocene age volcanic rocks as lenses, veins/veinlets, and fillings of pore spaces, vugs, cavities and fractures. The turquoise is mainly associated with other copper oxide and sulfide minerals such as malachite, azurite and chrysocolla and rarely chalcocite, covellite, pyrite and chalcopyrite. Turquoise mineral groups are hydrated phosphates with tricyclic crystalline systems. Its main formula is $AB_6(PO_4)_x(OH)_{2x}(OH)_8.4H_2O$ in which Ca, Cu^{2+}, Fe^{2+} and Zn substitute A and Al, Fe^{3+} and Cr^{3+} have the potential to replace B. Figure 2 shows the schematic structure of turquoise crystals with the chemical formula $CuAl_6(PO_4)_4(OH)_8 \cdot 4H_2O$ (Palache et al., 1944).

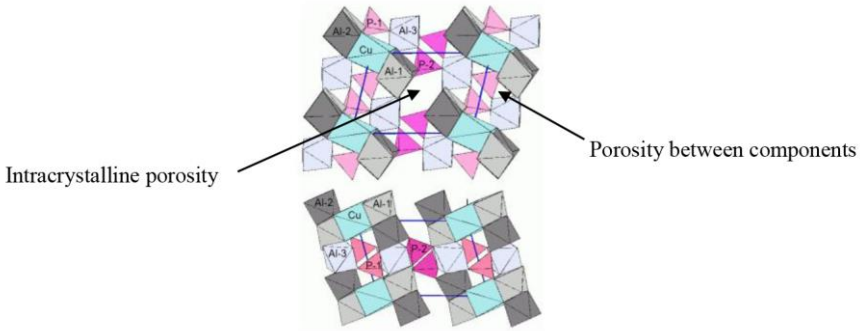

Fig. 2. Turquoise crystal structure (Palache et al., 1944)

2. Material and Methods

BET testing has several advantages such as being a non-destructive method for a sample and useful method for powder samples. Before testing, the sample was placed at a high temperature (>120°C) for several hours (2 or 3). The samples are routinely degassed and dehydrated at 120°C for 2 hours. Also, water vapor, carbon dioxide, or other molecules that may have occupied the volume of the material's cavities were removed. Some specimens, such as low-grade turquoises are damaged in these conditions. We controlled the conditions to prevent damage to samples. Two representative low-grade turquoise samples from Neyshabour mine were used for BET testing and treatment. To increase the effectiveness of the surface area, each sample was cut into beads. Specifications of the

studied samples are given in Table 1. About 0.1 gr of each sample was powdered at approximately 100 microns after degassing and placed in the cell of the measuring device. BET measuring was conducted at the Hesgar Mavad Saba research laboratory, Tehran, Iran. It is equipped with two Japanese Mini Belsorp devices. It is one of the most equipped and specialized BET laboratories in Iran and follows the most accurate analytical methods.

Table 1. Specifications of the studied samples

Sample code	Sample image	Sample weight	Sample color
NN-107		1.352 gr	Green
NN-108		0.963 gr	Blue White

3. Results and discussion

The surface area measurement, volume, and pore distribution have numerous applications in the research of catalysts, activated carbons, pharmaceuticals, ceramics, polymers, paints, coatings, nanotubes, minerals, and gems. Therefore, different methods for measuring surface area and porosity have been considered, such as microscopy and adsorption-based methods. If a solid such as gem is impermeable and completely stable, its total surface area can be approximated. But for porous structures, it is difficult to determine the amount of porosity and total area. One of the most important methods to accurately measure the total area of porous samples is the BET method which is based on the absorption of some specific molecular species in a gaseous state based on their surface (Brunauer, et al., 1938). Most solids have cavities inside their structure known as porosity and are classified by size, type, and shape. Porosity includes all pores, which are expressed as either total porosity or effective porosity. Total porosity consists of all the pores in the material, obtained from the ratio of the volume of the cavities to the total volume of the material. Effective or useful porosity consists of interconnected pores capable of passing fluids. This porosity is obtained from the ratio of the volume of interconnected pores to the total volume of material. Classification of cavities by International Union of Pure and Applied Chemistry[1] is given in Table 2. According to the classification by IUPAC, the structure of porous materials, depends on the average dimensions of the cavities. It can contain pores smaller than 2 nm, named micro-pores like zeolite porosities. The pores between 2 to 50 nm are known as meso-porous like silica porous. Some kinds of activated carbon and the pores larger than 50 nm are called macro-pores, such as metals and ceramics (Farrokh et al., 2019).

[1] IUPAC

Table 2. Classification of cavities by IUPAC

Pore size in nanometers	named
about 2 nm	micro-porous
2 nm to 50 nm	meso-porous
50 nm or more	macro-porous

In the porosity analysis, three factors are considered: surface area, volume, and size of the cavities. The specific surface area is the ratio of the total area of the porous body to its mass and the percentage of porosity is the ratio of the total volume of cavities to the total body volume. The basis for measuring porosity and surface area in this method is based on the adsorption of adsorbed material. Adsorption is the process of absorbing atoms or molecules in a liquid or gas in contact with a solid surface (Farrokh et al., 2019). This adsorption occurs by adhesion forces. If the conditions are taken to form a complete layer of molecules adsorbed on the surface, by determining the average thickness of a molecule, the surface occupying one molecule can be calculated. Thus, based on the amount of adsorbed material, the area of the entire sample surface can be measured (Farrokh et al., 2019). The most suitable materials for this purpose are gases or vapors of some material that have small molecular dimensions and can penetrate into pores of several tens of nanometers. Adsorption is measured at a constant temperature. The amount of adsorbed material is measured on the adsorbent surface at different relative pressures. Adsorption isotherms are mathematical relationships showing the amount of material absorbed on the surface (Gibson et al., 2020).

3.1. Types of adsorption isotherms

In addition to the cell containing the sample in the liquid nitrogen tank, the amount of gas absorbed by the material is calculated by gradually increasing the nitrogen gas pressure at each step. Then, by decreasing the gas pressure, desorption rate of the material is measured. Finally, the graph of the volume of nitrogen gas absorbed and desorbed by the substance is plotted at a constant temperature (Gibson et al., 2020). The results of the BET theory in 1985 are given in Figure 3. Based on the BET theory, the IUPAC adsorbed isotherms were divided into 6 categories. In other words, in physical adsorption, the adsorption isotherm can be classified into one of 6 general types below. Table 3 lists the types and characteristics of each graph (Brunauer et al., 1938; Taghi Malek et al., 2016).

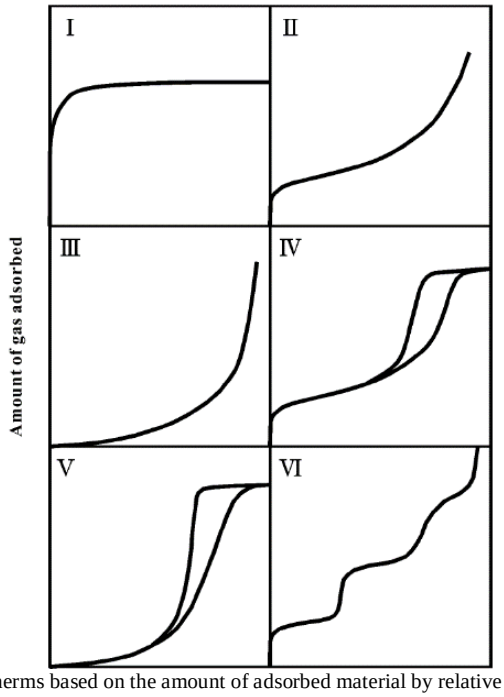

Fig. 3. Types of adsorption isotherms based on the amount of adsorbed material by relative pressure (Brunauer et al., (1938)

Table 3. Adsorption Isotherm Properties (Brunauer et al., (1938)

Type	features	
	Relationship between the sample surface and absorption rate	porosity
I.	Relatively strong	micro-porous
II.	Relatively strong	micro- porous
III.	weak	No holes
IV.	Relatively strong	meso- porous
V.	weak	meso- porous micro- porous
VI.	Relatively strong, sample surface even has an energy distribution	No holes

The BET theory was tested on the low grade turquoise of studied samples in our research and the results of the analysis are given in Fig. 4. The results were compared with the above standard diagrams. It can be concluded that their adsorption and desorption types are of the second type. According to Table 3, their adsorption is relatively strong. In general, if the value in diagrams plots below P_0 = 0.5, they are of a more micro-porous type. If they are above this point, the meso-porous types are higher (Brunauer et al., 1938). This is clearly indicated in the diagrams in (Figure 4).

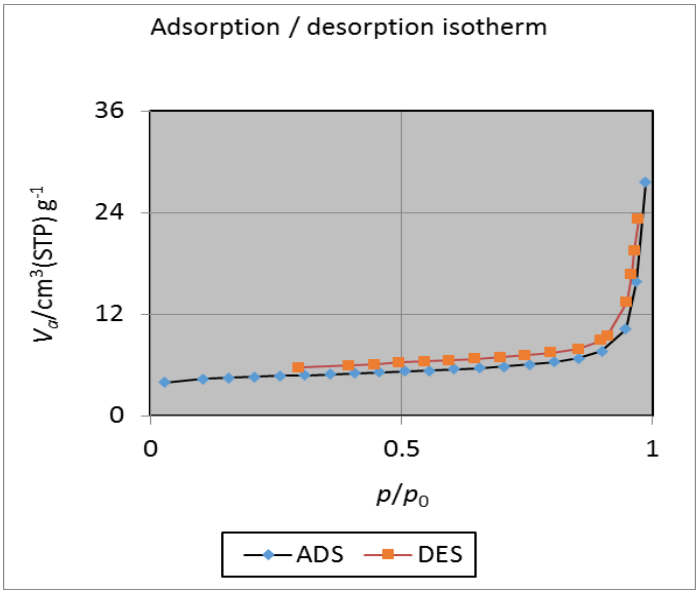

NN-107

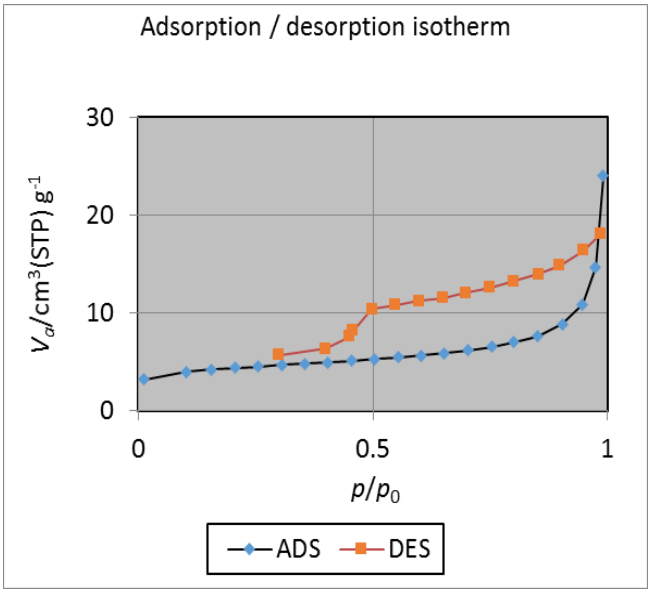

NN-108

Fig. 4. Absorption and desorption diagrams of the studied samples

3.2. Hysteresis space

The space created between the absorption and desorption diagrams is referred to as the hysteresis space. It indicates the presence of meso-porous in the sample and can be used to obtain information about the geometry of the cavities. In general, the higher the hysteresis space is, the higher the porosity levels are in the sample. Five types of hysteresis regarding with the shape of cavities are shown in Figure 5. It can be deduced from the diagrams, that the geometrical shape of the cavities in the samples above are cracks and open cylinders (Rouquerol et al., 2013).

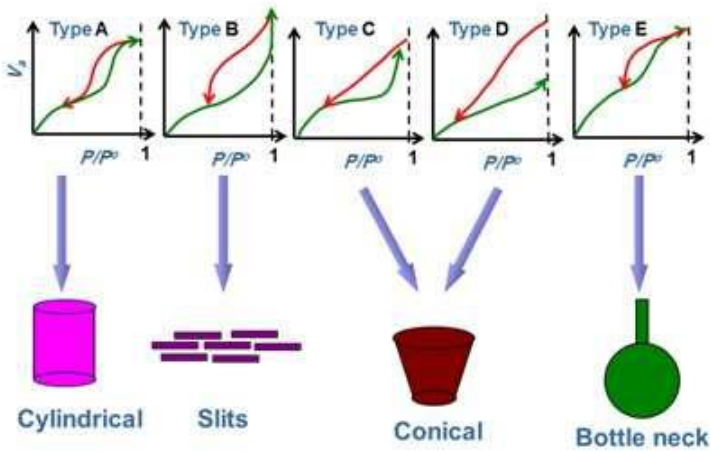

Fig. 5. Types of hysteresis according to cavity geometry (Rouquerol et al., 2013)

3.3. SEM analysis

In order to achieve high-resolution imaging from the upper-most surface of a specimen, we used SEM instrument with advanced detectors. The SEM used in this research was an FE-SEM (Hitachi SU 8230, Japan) equipped with different electron detectors. The advanced detectors are used to selectively detect electrons that are emitted locally at the point of interaction between the primary electron beam and the specimen surface. Basically, the detector which is placed directly under the thin specimen can be used for acquiring images in transmission mode in an SEM. In this research, the SEM was employed to observe the geometric structure of the porosity of samples. The samples were coated with carbon. SEM observations on the sample NN-107 show that the sample has been filled out by clay, has

dense cavities (micro-cavity), high porosity, and has low permeability (Welton, 1984). It was reported as indicated in section 3.1 and the P / P_0 ratio in Figure 4 and Figure 6. Also, SEM observations on the sample NN-108 show that the sample is a silicate which has been filled with clays and quartz nano-particles (Fig. 7).

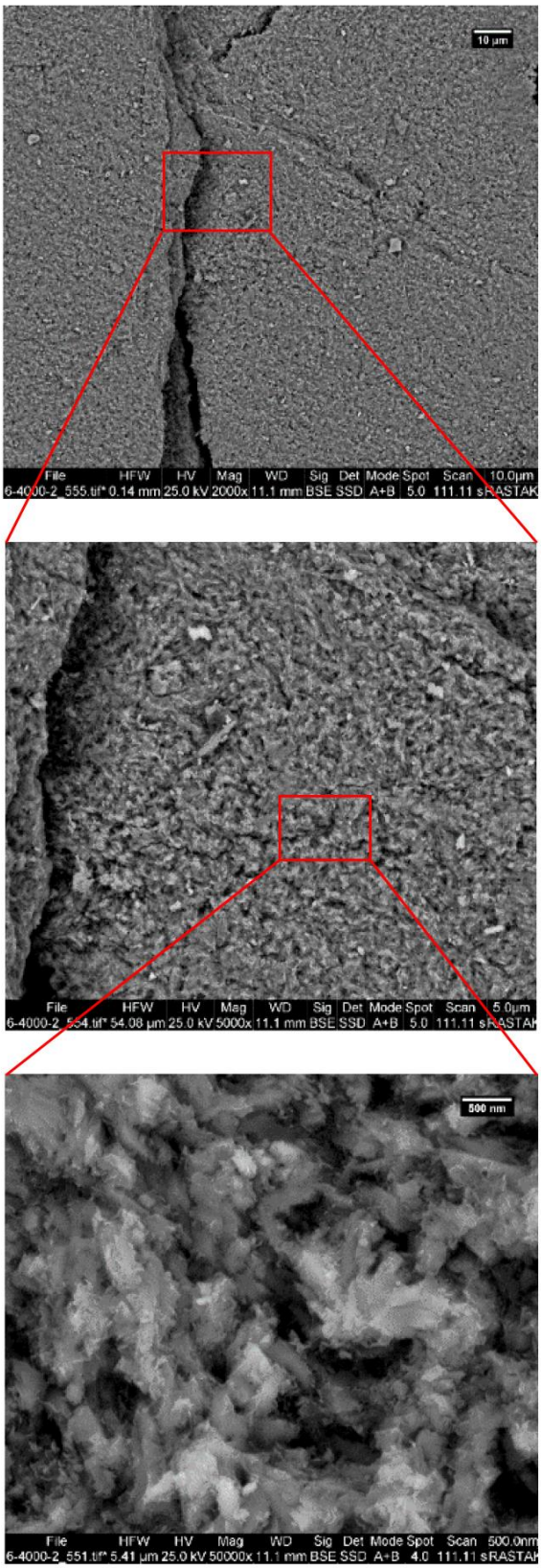

Fig. 6. Different magnifications of 10µ, 1µ and 500 nm on sample NN-107

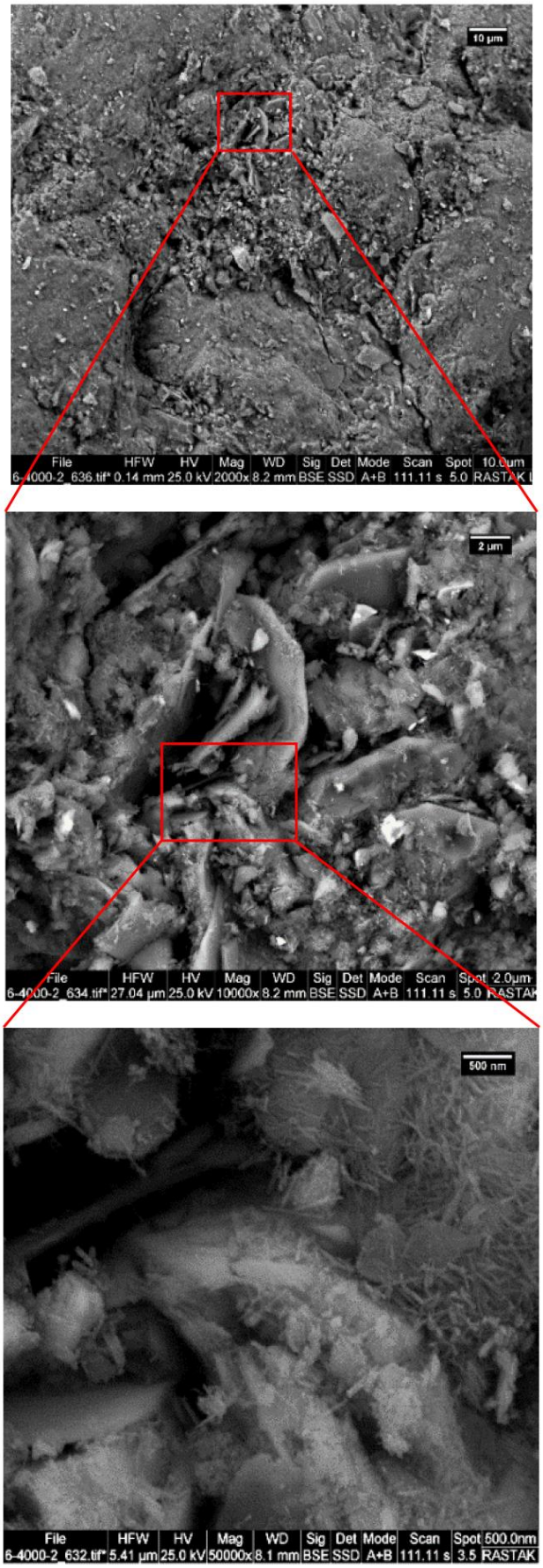

Fig. 7. Different magnifications of 10µ, 2µ and 500 nm on sample NN-108

3.4. Langmuir space

The Langmuir adsorption model describes the adsorption process by assuming the adsorbent behavior as an ideal gas under isothermal conditions (Lowell, et al., 2012). In calculating effective surfaces, we have a specific surface that contains surfaces that can absorb Nitrogen gas ($a_{s,BET}$). In addition, the Langmuir surface ($a_{s,Lang}$) as a general surface that can contain portions, includes no pores. Generally, if the surface of the sample is calculated by the Langmuir formula, it is referred to as the general surface ($a_{s,Lang}$). But if calculated by the BET formula, it is expressed as the specific surface ($a_{s,BET}$) in the results.

3.5. Determining the specific surface area and calculating of the porosity percentage

The specific surface area is the ratio of the total area of the porous body to its mass. In tables 4 and 5, the specific surface area ($a_{s, BET}$) values, as the effective surface area that this material can absorb as adsorbent, the maximum pore diameter ($r_{p, peak}$) and the total volume (V_m) are shown. These are separately expressed for each sample (Taghi Malek et al., 2016). The porosity percentage is calculated using the special surface according to this Formula:

Eq. 1. $$\%P = \frac{Vm}{as\ BET \times \rho} \times 100$$

The turquoise density was approximately between 2.6 gr/cm^3 - 2.8 gr/cm^3 but due to high water absorption of the samples, it was not possible to weigh them in water. For the above calculations, we use ρ = 2.7 gr/cm^3 as the mean density.

$\%P_{NN\text{-}107} = \frac{3.891}{16.935 \times 2.7} \times 100 = 8.5\%$, $\%P_{NN\text{-}108} = \frac{3.6034}{15.684 \times 2.7} \times 100 = 8.5\%$

Table 4. BET test results for sample NN-107

NN- 107		
BET plot		
V_m	3.891	[cm^3(STP) g^{-1}]
$a_{s,BET}$	16.935	[m^2 g^{-1}]
Total pore volume(p/p0=0.986)	0.042679	[cm^3 g^{-1}]
Average pore diameter	10.08	[nm]
t plot		
Plot data	Adsorption branch	
a_1	19.32	[m^2 g^{-1}]
V_1	0	[cm^3 g^{-1}]
a_2	9.5767	[m^2 g^{-1}]
	-0.00054356	
V_2	-0.11089	[cm^3 g^{-1}]
2t		[nm]
BJH plot		
Plot data	Adsorption branch	
V_p	0.036067	[cm^3 g^{-1}]
	22.07	
$r_{p,peak(Area)}$		[nm]
A_p	4.8154	[m^2 g^{-1}]

Table 5. BET test results for sample NN-108

NN- 108		
BET plot		
V_m	3.6034	$[cm^3(STP)\ g^{-1}]$
$a_{s,BET}$	15.684	$[m^2\ g^{-1}]$
Total pore volume(p/p0=0.986)	0.03678	
Average pore diameter	9.3806	$[cm^3\ g^{-1}]$ [nm]
t plot		
Plot data	Adsorption branch	
a_1	17.931	$[m^2\ g^{-1}]$
V_1	0	$[cm^3\ g^{-1}]$
a_2	8.2445	$[m^2\ g^{-1}]$
V_2	0.0027636	
2t	0.5671	$[cm^3\ g^{-1}]$ [nm]
BJH plot		
Plot data	Adsorption branch	
V_p	0.032116	$[cm^3\ g^{-1}]$
$r_{p,peak(Area)}$	1.64	[nm]
A_p	4.8468	$[m^2\ g^{-1}]$

Another way to calculate porosity percentage according to formula 2 is to calculate the ratio of the porosity volume to total volume.

Eq. 2. $\%P = \frac{Vp}{Vm} \times 100$

Therefore, according to the above formula, the porosity percentage of each sample is:

$\%P_{NN\text{-}107} = \frac{0.036067}{3.891} \times 100 = 0.92\ \%$, $\%P_{NN\text{-}108} = \frac{0.032116}{3.6034} \times 100 = 0.89\ \%$

By comparing the two samples with each other, we notice that the effective porosity of both samples are approximately same and the difference in the results is due to the inability to accurately calculate the density of the samples. According to the data presented in Tables 4 and 5, the largest pore diameter in sample NN-107 was 22 nm. According to the information in Table 2, the porosity is meso-porous. Also in sample NN-108, the greatest pore diameter was 1.2 nm and the porosity is in the form of micro-porous.

3.6. Other methods

The T-plot method is a well-known technique that allows the comparison of micro-porous or meso-porous samples and the specific surface area of each sample with the reference adsorption isotherm of a non-porous material with the same surface chemistry (Lowell et al., 2012). In this section two surfaces are mentioned in which a_1 is the general special surface and is also known as the internal surface and a_2 or the external surface which a_1 is usually an approximate equal of BET. Therefore, according to formula 3, the micro level is always equal to:

Eq. 3. $a_{micro} = a_{1\ total} - a_{2\ external}$

BJH (Barrett, Joyner and Halenda) method can be used to determine pore surface area and volume, using adsorption and desorption techniques. In 1951, Barrett et al. proposed a computational method to obtain the cavity size distribution from the adsorption isotherm data and named it BJH (Lowell et al., 2012).

4. Conclusion

Using physical adsorption and accurate analysis of the BET results, we can obtain useful information such as specific surface area, porosity volume, and cavity size distribution. Before obtaining the above information, the examination of the isothermal diagram (adsorption and desorption isotherm) will give a fairly good understanding of the shape of the cavities. Finally, using the

isotherm shape, the type of cavities will be determined in terms of micro-porous, meso-porous or macro-porous. The results are essential information for gemstone treatment. Estimation of the shape of the cavities can be obtained by examining the results of the form of isothermal adsorption and desorption curves (BET). The BET analysis of the samples analyzed in this research show that their adsorption and desorption type is of the second standard type of IUPAC diagrams and their adsorption is relatively strong. SEM observations on the samples NN-107 and NN-108 show that the sample NN-107 has dense cavities (micro-cavity), high porosity, and has low permeability once compared with sample NN-108. The sample NN-108 has less porosity due to the presence of quartz nano-particles which are filled out by clay. The result of the analysis in this research show that the geometrical shape of porosity is two sided and of open cylindrical type. The porosity is mainly of micro-pore type ($P_0 \leq 0.5$) and the absorption is a high type. Therefore, treatment of the low-grade turquoise is fairly possible and makes it possible for further chemical treatment investigations.

Acknowledgement

The authors would like to express their deepest gratitude to all of the peoples who helped us to do this research in the laboratory of the Gemological Development Institute of Iran at Shahid Beheshti University and Dr. Farghdani, in the Hesgar Mavad Saba research laboratory.

References

Mortimer, C., 1746. XVII. Some remarks on the precious stone called the turquoise. Philosophical Transactions of the Royal Society of London, v. 44(482), p.429-432.

Afshar, I., 2004. Javaher Nameh Nezami (6th century), Mirass Maktub Press, 4464 p (in Persian).

Ghorbani, M., 2003. Precious minerals and stones in Iran, Iran Aryan Press, 420 p (in Persian).

Hajalilu, B., 2007. Gemology, Payam Noor Press, 340 p (in Persian).

Pogue, J.E., 1915. The turquoise: a study of its history, mineralogy, geology, ethnology, archaeology, mythology, folklore, and technology (v. 12). National Academy of Sciences.

Hazen, R.M., 1984. Mineralogy: A historical review. Journal of Geological Education, v. 32(5), p. 288-298.

Reyahi, M.A., 1963. Jahan Nameh (about Avecina), Avecina Press, 164 p (in Persian).

King, R.J., 2002. Turquoise. Geology Today, v. 18(3), p. 110-114.

Isfahani Sheikh, M. 1860. Javaher Nameh (Gemology), 54 p (in Persian).

Sotoodeh, M., 1954. Gohar Nameh (Gemology), Iran culture Press, 302 p (in Persian).

Akrami, M.R., Yazdi, M., Masoudi, F. and Delpasand, Z., 2019. Comparison of gemology and Raman spectroscopy between Neyshabour and Kerman low-grade turquoises, 22nd Symposium of Geological Society of Iran, p. 9-18 (in Persian).

Akrami, M.R., Yazdi, M., Masoudi, F. and Nojavan, S., 2020. The effective porosity and surface area determination of Neyshabour low-grade turquoises by BET method, Conference on Iranian gemstone deposits, p. 49-61 (in Persian).

Yazdi, M., 2008. Crystallography, Ball Press, 192 p (in Persian).

Garajian, O. and Lotfi, F., 2014. Turquoise Archeology: Man, Stone and Color. Iranian Anthropological Research, v. 4(2), p. 105-124 (in Persian).

Zalinski, E.R., 1907. Turquoise in the Burro Mountains, New Mexico. Economic Geology, v. 2(5), p. 464-492.

Zavosh, M., 1969. Mineralogy in ancient Iran, Iran culture foundation press, 344 p (in Persian).

Ovissi, M., Yazdi, M. and Ghorbani, M., 2015. Turquoise gemology of Iran in historical times (in old texts of Iran and world), 3th National meeting of gemology and crystallography of Iran, p. 18-25 (in Persian).

Ovissi, M., Yazdi, M. and Ghorbani, M., 2017. The Persian turquoise mining at Neyshabour mine in historical times, Journal of geography of Iran, v. 14(50), p. 87-99 (in Persian).

Gibson, N., Kuchenbecker, P., Rasmussen, K., Hodoroaba, V.D. and Rauscher, H., 2020. Volume-specific surface area by gas adsorption analysis with the BET method. In Characterization of Nanoparticles, p. 265-294. Elsevier.

Rezaei, M.H., Soleymani, S. and Ahmadi, K., 2016. Bishiklik petroglyphs in Neyshabur county, northeastern Iran. International Journal of Archaeology, v. 4(11).

Baumann, A., Spies, O. and Lensch, G., 1984. Strontium isotopic composition of post-ophiolitic Tertiary volcanics between Kashmar, Sabzevar and Quchan/NE Iran. Neues Jahrbuch für Geologie und Paläontologie-Abhandlungen, p. 409-416.

Spies, O., Lensch, G. and Mihem, A., 1983. Chemistry of the post-ophiolitic tertiary volcanics between Sabzevar and Quchan / NE-Iran. Geodynamic project (geotraverse) in Iran, Final report, Geo. Suv of Iran, Report, (51).

Akrami, M. and Asgari, A., 2000. 1: 100000 geological map of Soltanabad, Geological Survey of Iran.

Karimpour, M.H., Malekzadeh Shafaroudi, A., Esfandiarpour, A. and Mohammadnejad, H., 2012. Neyshabour Turquoise Mine: The first copper, gold, uranium and REE IOCG mineralization type in Iran, Journal of Economic Geology, v. 3(2), p. 193-216 (in Persian).

Palache, C., Frondel, C., Dana, J.D., Dana, E.S. and Berman, H., 1944. The System of Mineralogy: Of James Dwight Dana and Edward Salisbury Dana, Yale University 1837-1892. John Wiley & Sons.

Brunauer, S., Emmett, P.H. and Teller, E., 1938. Adsorption of gases in multimolecular layers. Journal of the American chemical society, v. 60(2), p. 309-319.

Farrokh, P.F., Mofarrah, E. and Nik khesal, R., 2019. Familiarity with surface analysis based on physical absorption and excretion. Iranian Journal of Laboratory Knowledge Quarterly, v. 6 (4), p. 7-12 (in Persian).

Taghi Malek, H., Marki, M. and Azargaman, M., 2016. Methods of measuring porosity and effective surface area. Shaaa scientific and specialized Quarterly, v. 2(2), p. 55-65 (in Persian).

Rouquerol, J., Rouquerol, F., Llewellyn, P., Maurin, G. and Sing, K.S., 2013. Adsorption by powders and porous solids: principles, methodology and applications. Academic press.

Welton, J.E., 1984. SEM petrology atlas.

Lowell, S., Shields, J.E., Thomas, M.A. and Thommes, M., 2012. Characterization of porous solids and powders: surface area, pore size and density (v. 16). Springer Science & Business Media.